Article:
Diaz-Cereceda, C., Hetherington, J., Poblet-Puig, J. et al. (2011) A deterministic model of impact noise transmission through structural connections based on modal analysis. Journal of Sound and Vibration, 330 (12). pp. 2801-2817. ISSN: 0022-460X

https://doi.org/10.1016/j.jsv.2010.12.019

A deterministic model of impact noise transmission through structural connections based on modal analysis

C. Díaz-Cereceda*[1], J. Hetherington†[2], J. Poblet-Puig‡[1] and A. Rodríguez-Ferran§[1]

[1]Laboratori de Càlcul Numèric, E.T.S. d'Enginyers de Camins, Canals i Ports de Barcelona, Universitat Politècnica de Catalunya
[2]Department of Civil and Structural Engineering. University of Sheffield. Mappin Street, Sheffield S1 3JD, United Kingdom

Abstract

Vibration transmission through structural connections is modelled in a deterministic way by means of modal analysis. This model is used first to study the effect of elastic joints across the floor in the transmission of impact noise. They are an effective means of reducing impact noise propagation, and can almost eliminate it for small values of the joint stiffness. The method is also used to study the acoustic relevance of studs in lightweight floor transmission. Different ways of modelling the studs are presented and compared. For the examples developed, the best option is to use springs for modelling the studs rather than more complex models involving springs and beams. Also the different behaviour of point and line connections is verified, as well as the influence of the position of the studs.

Keywords: modal analysis, impact noise, vibration level difference.

1 Introduction

Impact noise is an important parameter in acoustic building design. For this reason, models that provide the impact noise level for different types of floors are necessary. These models should be able to provide a description of vibration propagation, which

*e-mail:cristina.diaz.cereceda@gmail.com
†e-mail: cip09jeh@sheffield.ac.uk
‡correspondence: UPC, Campus Nord B1, Jordi Girona 1, E-08034 Barcelona, Spain, e-mail: jordi.poblet@upc.edu
§e-mail: antonio.rodriguez-ferran@upc.edu

is restricted by regulations and also required for computing impact noise levels. They should also cover a wide frequency range in order to evaluate the outputs defined in regulations (for instance $L_{\mathrm{n,w}}$ defined by ISO 717-2:1997 [1] requires frequencies from 100 Hz to 3150 Hz).

In this paper, the main objective is to compute the impact noise level L_{n} and the vibration transmission through structural connections (for instance calculating the vibration level difference D_{ij}) for some floor typologies.

There are two fundamental ways of solving a vibration problem. The first approach consists on solving it with energy average methods, as the Statistical Energy Analysis (SEA). Vèr [29] uses energy fluxes for the computation of impact noise. The bases of SEA for dealing with dynamical systems are described by Lyon in [22]. Some SEA models for impact noise can be found in the literature, as the models developed by Craik *et al.* in [11, 10, 9].

The second method consists on describing the problem deterministically and solving the dynamics equation by means of numerical methods. One option is to discretise the impacted structure with the Finite Element Method (FEM) as Rabold *et al.* do in [24]. Also, for simple geometries, the equation can be solved with modal analysis, as shown by Chung and Emms [8], Sjökvist *et al.* [26, 27] and Berry *et al.* [5] for homogeneous floors with different boundary conditions.

The computation of the impact noise can be done by integrating the sound intensity in the floor or through different techniques that make assumptions on the characteristics of the impacted floor and the propagation medium in order to derive simplified expressions of the radiation efficiency. Examples of these simplifications are the expressions provided by Fahy in [13] for small dimensions of the floor or the simplifications given by Renji *et al.* [25] for aspect ratios of the rectangular plate close to 1.

In this work, a deterministic and decoupled approach to the vibroacoustic problem is performed. It consists on modelling first the applied force, then computing the velocity field of the floor caused by that force assuming time-harmonic dependence and finally obtaining the power radiated by the vibrating floor, required to compute the standard magnitudes for the impact noise measurement. The force is calculated as described in [6]. The dynamics equation is solved with modal analysis, since for simple geometries (as the rectangular plates considered here) this technique has a reasonable computational cost even for a wide range of frequencies.

The main contributions of this paper are:

- A formulation that accounts for the vibration transmission through the border of linked rectangular plates (Section 3). The vibration field in the plates is described by means of a modal expansion and the coupling between them is accounted in the variational formulation of the problem. Eigenfunctions of a rectangular plate with different boundary conditions can be considered with the only restriction that rotations must not be blocked in the vibration transmission border. The formulation has been used in order to calculate the propagation of vibrations caused by the impact tapping machine through floors/structures composed of several rectangular plates.

- The analysis of the potential effect of an elastic joint on the vibration transmis-

sion through the structures mentioned above (Section 3).

- The prediction of the vibration response of lightweight floors composed of rectangular plates connected by means of studs (Section 4). A generalisation of existing modal approaches to this kind of floors [8, 27] has been used in order to:

    1. Compare several modelling options of the connecting element (stud) depending of its floor stiffening effect and its cross-section flexibility. Each of the three proposed models is adequate for a different stud typology.
    2. Analyse the relevance of the connection between the stud and the plate. The differences in the vibration transmission depending on the separation of the screws that connect the studs and the leaves of the floor are shown (and quantified). This is an important aspect when deciding if line or point connecting springs are more adequate in simplified models and how should the stiffness of these elements be assigned.

An outline of the paper follows. The basis of the model is presented in Section 2. The enrichment mechanisms for dealing with flanking transmission problems are described in Section 3. Also the formulation for dealing with lightweight floors is described in Section 4. Some comparisons with experimental data and other models are presented in Section 5, as well as some results derived from the models. Concluding remarks of Section 6 close the paper.

2 Basis of the model

The goal of this model is to analyse the impact noise transmission through structural connections between floors, using a modified formulation of the modal analysis. On the one hand flanking transmission between floors interconnected through the plate edge is modelled, and on the other hand the vibration level difference between leaves that are part of lightweight floors is computed.

The impact noise is measured with the normalised impact noise pressure level L_{n}, as defined in ISO 140-6 [2]. This value requires the floor to be excited by the normalised tapping machine [2] and can be computed in terms of the power radiated by the floor as (see Brunskog and Hammer [7])

$$L_{\mathrm{n}} = 10 \log_{10} \left(\frac{\Pi_{\mathrm{rad}}}{p_{\mathrm{ref}}^2} \frac{4\rho c}{A_0} \right) \mathrm{dB}, \tag{1}$$

where A_0 is the reference absorption area (10 m^2 for dwellings), Π_{rad} the radiated power, p_{ref} the reference pressure (2×10^{-5} Pa), ρ the air density and c the speed of sound in the air.

The structural part of the problem is modelled with the thin plate equation in the frequency domain

$$D\Delta^2 u - \omega^2 \rho_s u = q \tag{2}$$

where

$$D = \frac{E(1+\mathrm{i}\eta)h^3}{12(1-\nu^2)}$$

is the complex bending stiffness of the plate, E Young's modulus, $\mathrm{i} = \sqrt{-1}$ the imaginary unit, ν Poisson's ratio, h the thickness of the plate, η the loss factor as defined in [4], ρ_s the mass per unit surface, q the applied load per unit surface, $\omega = 2\pi f$ (with f the frequency of vibration) and $u(x, y)$ the displacement phasor.

For the case of a rectangular plate simply supported along its edges without external moments applied, the displacement is expressed in terms of the eigenfunctions ψ_{pq} as

$$u(x, y) = \sum_{p,q}^{M} a_{pq}\, \psi_{pq}(x, y) \tag{3}$$

where a_{pq} is the modal contribution of mode ψ_{pq}, M is the number of modes per plate,

$$\psi_{pq} = \sin\left(\frac{p\pi}{L_x}x\right) \sin\left(\frac{q\pi}{L_y}y\right) \tag{4}$$

and L_x, L_y are the lengths of the sides of the plate in x and y directions respectively.

This basis of functions is used all over the paper as it is a good interpolation basis for the cases considered, where the plates are supposed to have null displacements along the edges. If the conditions about the displacements and rotations in the plate edge were different, other eigenfunctions can be used, as done in Section 5.3.3.

Eq. (3) can be replaced in the weak form of the differential equation (2) using Galerkin formulation, and the values of a_{pq} are obtained solving a linear system. For the case of a simply supported plate without any external moments, this system is diagonal and each value a_{pq} can be computed explicitly as described by Graff [17] (the exact expression appears in [20]).

The displacements of the plate can be found then with Eq. (3), and the velocity of the plate is obtained as $v(x, y) = \mathrm{i}\,\omega\, u(x, y)$.

Once the vibration field is computed, the power radiated by the excited plate can be calculated as

$$\Pi_{\mathrm{rad}} = \int_s I \cdot \mathrm{d}s = \frac{1}{2}\mathrm{Re}\left(\int_s pv^* \mathrm{d}s\right) \tag{5}$$

where I is the sound intensity and pv^* the product of the acoustic pressure and the conjugate velocity phasor over the integration surface.

Using the expression of acoustic pressure in a semi-infinite space proposed in [13]

$$p(x, y, z = 0^+) = -\frac{\mathrm{i}\omega\rho}{2\pi}\int_0^{L_y}\int_0^{L_x} v(x', y')\frac{\mathrm{e}^{\mathrm{i}kr}}{r}\mathrm{d}x'\mathrm{d}y', \tag{6}$$

where $z = 0$ is the source plane and $r = \left[(x-x')^2 + (y-y')^2\right]^{1/2}$ and replacing Eq. (6) in Eq. (5) as proposed by Williams [30], the radiated power is expressed in terms of the plate surface velocity as

$$\Pi_{\mathrm{rad}} = \frac{\omega\rho}{4\pi}\int_{\Omega'}\int_{\Omega} v(x', y')v^*(x, y)\frac{\sin(kr)}{r}\,\mathrm{d}\Omega\,\mathrm{d}\Omega' \tag{7}$$

where $k = \omega/c$ is the wavenumber in the air at the given frequency and Ω, Ω' are used to denote the double integral over the plate.

This integral is calculated numerically with the trapezoidal composite rule, using 8 nodes per wavelength (the integration points vary with ω).

Alternatively, analytical expressions of the radiation efficiency of a rectangular plate are found in the literature. They are obtained by means of the wave approach or modal analysis and avoid the integrals of Eq. (7). However, they only apply for certain geometrical configurations of the plates. This is the case of the expressions shown by Renji *et al.* [25], only valid for aspect ratios close to 1, used here to compute powers for large frequencies, where they have been proven to provide the same results as the integral of Eq. (7).

Once the radiated power is computed, L_{n} can be obtained with Eq. (1). Then, the adjusted normalised impact noise pressure level ($L_{\mathrm{n,w}}$) can be computed as defined by the ISO 717-2:1997 [1]. This parameter is useful for establishing simple comparisons between different floors.

In the following two sections the interest is focused on the modelling of different floors, in order to obtain the velocity field required by Eq. (7).

3 Flanking transmission

The first model developed deals with the computation of flanking transmission of impact noise in continuous floors with elastic joins between spans, see Fig. 3. The goal is to compute the impact noise generated by every plate, when the force is applied only in one of them.

The impact is caused by the tapping machine and is modelled as detailed by Brunskog and Hammer [6]. The behaviour of the machine depends on the properties of the contact surface. There are two limit situations in this behaviour. One of them is the case of the hammers rebounding with the same velocity of the impact (elastic behaviour). In the other limit situation the hammers do not rebound at all (damped behaviour).

The formulation proposed in [6] takes into account the fact that the floor may have an intermediate behaviour between these two limits. It provides the spectrum of the force exerted by the tapping machine $F_0(f)$ for a floor of known properties, with

$$F_0(f) = \sum_{n=-\infty}^{\infty} F_n \delta(f - n f_r) \tag{8}$$

with $F_n = F_1(n f_r) f_r$, $f_r = 10\,\mathrm{Hz}$ and

$$F_1 = \begin{cases} \frac{v_0 K M}{K - \omega^2 M + \mathrm{i}\omega K M/R} & \text{for } KM \geq 4R^2 \\ \frac{v_0 K M \left(1 + e^{-t_{\mathrm{cut}}(\mathrm{i}\omega + K/2R)}\right)}{K - \omega^2 M + \mathrm{i}\omega K M/R} & \text{for } KM < 4R^2 \end{cases} \tag{9}$$

where:

- v_0 is the speed with which the hammer hits the plate and its value is $v_0 = (2gh_0)^{1/2} = 0.866\,\mathrm{m\,s^{-1}}$ as the hammer is dropped from a height of 0.04 m.

- K is the stiffness of the local deformation. It can be approximated by the static deformation caused by a rigid stamp on a semi-infinite elastic solid (Boussinesq deformation)
$$K = ED_h/\left(1-\nu^2\right). \tag{10}$$
- D_h is the diameter of the hammer (0.03 m according to the ISO 140-7:1998 [3]).
- M is the mass of each hammer.
- R is a measure of the resistance and is assumed to be due to energy transportation within the plate. It may be expressed as the input impedance of an infinite plate
$$R = 8\sqrt{\rho_s B}. \tag{11}$$
- $t_{\text{cut}} = \pi\sqrt{\frac{M}{K}}$ is the time of zero-crossing.

3.1 Elastic joints: meaning and modelling

The elastic joint controls the transmission of bending moment between plates. The constitutive equation chosen for a joint parallel to the y axis is

$$M = k_\theta(\theta_1 - \theta_2) \tag{12}$$

where k_θ is the rotation stiffness of the joint, θ_1 and θ_2 are the rotations of the two plates at their common side defined as

$$\theta_1 = \left.\frac{\partial u_1}{\partial x_{(1)}}\right|_{x_{(1)}=L_{x1}}, \qquad \theta_2 = \left.\frac{\partial u_2}{\partial x_{(2)}}\right|_{x_{(2)}=0},$$

L_{x1} is the length of the first plate in the x direction and M is the bending moment per unit length as shown in Fig. 1.

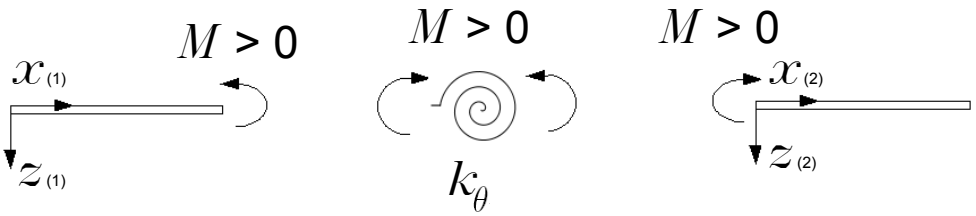

Figure 1: Sign criterion for positive bending moments in an elastic joint

This formulation allows to take into account the joint damping loss factor by using a complex value of the rotational stiffness $k'_\theta = k_\theta\,(1+\eta\mathrm{i})$.

The physical meaning of the rotational stiffness k_θ depends on the particular properties of the real linking device or joint material. For an elastic material a 2D analysis can be performed, which leads to a value of $k_\theta = \frac{Eh^3}{12a}$ where E is the young modulus of the material forming the joint, h the height of the joint and a its thickness (see Fig. 2).

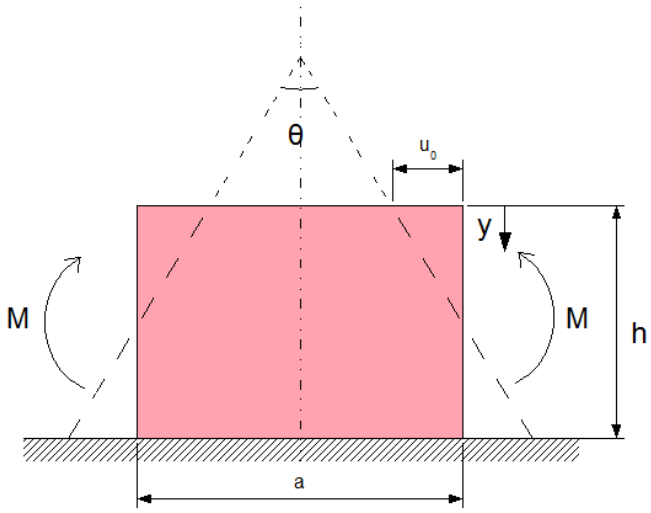

Figure 2: Analysis of the elastic joint rotation stiffness

Since for plates with joints at their boundaries the functions in Eq. (4) are no longer eigenfunctions, the conditions shown in Eq. (12) should be imposed weakly in the differential equation. For this reason, the following development of the weak form of Eq. (2) is chosen:

Let W be the space of functions whose value is zero at the boundary of the domain $\partial\Omega$. Then, the boundary value problem can be stated as follows:

Find a function $u \in W$ such that for all $w \in W$

$$D\int_\Omega \Delta^2 w\, u\,\mathrm{d}\Omega - D\int_{\partial\Omega} \Delta u \nabla_n w\,\mathrm{d}\Gamma + D\int_{\partial\Omega} \Delta w\,\nabla_n u\,\mathrm{d}\Gamma - \\ - \omega^2\rho_s\int_\Omega uw\,\mathrm{d}\Omega = \int_\Omega qw\,\mathrm{d}\Omega. \quad (13)$$

The same basis of functions defined in Eq. (3) is used in order to do the modal expansion of the displacement. Because of this, in Eq. (13) the first term can be rewritten using $\Delta^2 w = k_{pq}^4 w$ and joined with the fourth one. Also, the third term vanishes because $\Delta w = -k_{pq}^2 w$ and w is null at $\partial\Omega$. If, in addition to this, the second term is written in terms of the bending moment, Eq. (13) becomes

$$\int_\Omega \left(Dk_{pq}^4 - \omega^2\rho_s\right) u\, w\,\mathrm{d}\Omega - \left(\int_0^{L_y} M_x \frac{\partial w}{\partial x}\,\mathrm{d}y\right)_{x=0} + \left(\int_0^{L_y} M_x \frac{\partial w}{\partial x}\,\mathrm{d}y\right)_{x=L_x} - \\ - \left(\int_0^{L_x} M_y \frac{\partial w}{\partial y}\,\mathrm{d}x\right)_{y=0} + \left(\int_0^{L_x} M_y \frac{\partial w}{\partial y}\,\mathrm{d}x\right)_{y=L_y} = \int_\Omega q\, w\,\mathrm{d}\Omega. \quad (14)$$

This equation should be imposed for each plate forming the floor. Terms from 2 to 5 are related to the bending moments applied on the boundary of the plate. These moments are zero for simply supported edges and can be expressed as shown in Eq. (12) for joints. For Fig. 3, plates 1 and n have one of those terms different from zero and the rest of plates have two.

The right hand side term is only different from zero at those plates where an external force is applied. Replacing w by ψ_{lm} and u by the modal expansion of each

plate, equations become a linear system whose solutions are modal contributions a_{pq} for each plate.

3.2 Vibration transmission in continuous floors

The case of Fig. 3 is considered: various floor spans connected by elastic joints. This is a proposal of acoustic improvement for continuous floors in edification.

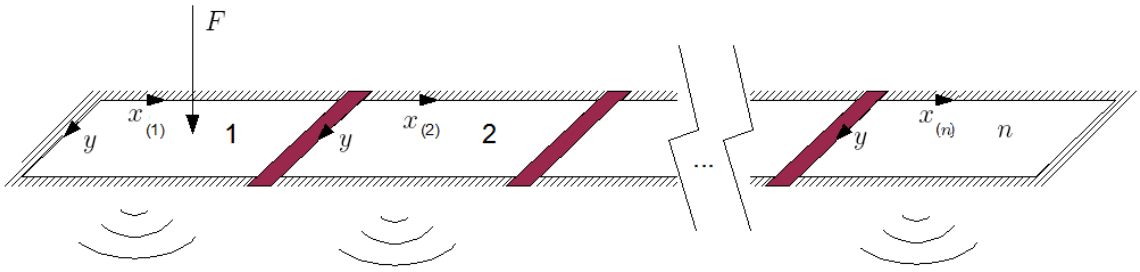

Figure 3: Impact noise for continuous floors

The aim here is to simulate the usual situation in buildings, where the vibration transmission depends on the connections between floors.

After substituting the boundary conditions in the weak form and computing the integrals, linear system (15) yields

$$\mathbf{K}\mathbf{a} = \mathbf{f} \tag{15}$$

where

$$\mathbf{K} = \begin{bmatrix} \mathbf{D_{11}}+k_\theta\mathbf{B_{11}} & -k_\theta\mathbf{B_{12}} & & & \\ -k_\theta\mathbf{B_{21}} & \mathbf{D_{22}}+2k_\theta\mathbf{B_{22}} & -k_\theta\mathbf{B_{23}} & & \\ & -k_\theta\mathbf{B_{32}} & \ddots & \ddots & \\ & & \ddots & \ddots & -k_\theta\mathbf{B_{N-1,N}} \\ & & & -k_\theta\mathbf{B_{N,N-1}} & \mathbf{D_{NN}}+k_\theta\mathbf{B_{NN}} \end{bmatrix}$$

$$\mathbf{a} = \begin{Bmatrix} \mathbf{a_1} \\ \mathbf{a_2} \\ \vdots \\ \vdots \\ \mathbf{a_N} \end{Bmatrix} \qquad \mathbf{f} = \begin{Bmatrix} \mathbf{f^{ext}} \\ \mathbf{0} \\ \vdots \\ \vdots \\ \mathbf{0} \end{Bmatrix}$$

where $\mathbf{a_1}$, $\mathbf{a_2}$, ..., $\mathbf{a_N}$ are vectors with the modal contributions of plates $1, 2, ..., N$ respectively.

The global matrix is block-tridiagonal, as each plate is connected, at most, to two other plates. Each block matrix has size $M \times M$ and vectors $\mathbf{a_i}$ and $\mathbf{f^{ext}}$ have dimension M, where M is the number of modes per plate.

Matrices $\mathbf{D_{ii}}$ correspond to the first term of Eq. (14). They are diagonal due to the orthogonality of the functions and their diagonal entries are $\left(Dk_{pq}^4 - \omega^2\rho_s\right)\int_\Omega \psi_{pq}\psi_{pq}\mathrm{d}\Omega$.

Matrices $\mathbf{B_{ij}}$ derive from the replacement of Eq. (12) in the weak form, Eq. (14). Each of these terms provides two block matrices (due to the subtraction appearing in the constitutive equation), whose elements are of the form

$$\int_{y=0}^{y=L_y} \frac{\partial \psi_{pq}}{\partial x_{(i)}} \frac{\partial \psi_{lm}}{\partial x_{(j)}} \mathrm{d}y, \tag{16}$$

where i and j are the numbers of the plates involved. These are full matrices, as the derivatives of the shape functions do not satisfy orthogonality.

3.3 Vibration transmission in T-shaped joints

The case of Fig. 4 is also modelled: a T-shaped structure based on three simply supported plates with a common side where the displacements are null but the rotations are linked by means of an elastic joint. This is representative of the intersection of a floor and a wall in edification.

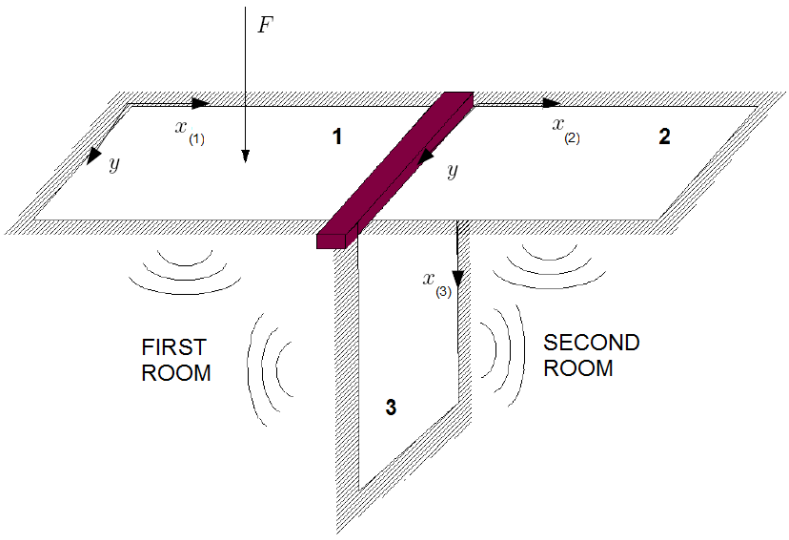

Figure 4: Impact noise for a T-shaped structure

The aim of this model is to take into account the wall vibration when computing the impact noise.

In this case the effect of the joint is represented by three different stiffnesses: $k_{\theta 12}$ is the stiffness between the two floors, $k_{\theta 13}$ is the stiffness between the first floor and the wall and $k_{\theta 23}$ is the stiffness between the second floor and the wall.

In this model the output of interest is the impact noise pressure level in the first and second rooms. The impact noise in rooms is computed adding, for each room, the power radiated by the floor above and the power radiated by the wall.

After substituting the boundary conditions in the weak form and computing the integrals the linear system (17) yields

$$\mathbf{Ka} = \mathbf{f} \tag{17}$$

where

$$\mathbf{K} = \begin{bmatrix} \mathbf{D_{11}}+(k_{\theta 12}+k_{\theta 13})\mathbf{B_{11}} & -k_{\theta 12}\mathbf{B_{12}} & -k_{\theta 13}\mathbf{B_{13}} \\ -k_{\theta 12}\mathbf{B_{21}} & \mathbf{D_{22}}+(k_{\theta 12}+k_{\theta 23})\mathbf{B_{22}} & -k_{\theta 23}\mathbf{B_{23}} \\ -k_{\theta 13}\mathbf{B_{31}} & -k_{\theta 23}\mathbf{B_{32}} & \mathbf{D_{33}}+(k_{\theta 23}+k_{\theta 13})\mathbf{B_{33}} \end{bmatrix}$$

$$\mathbf{a} = \begin{Bmatrix} \mathbf{a_1} \\ \mathbf{a_2} \\ \mathbf{a_3} \end{Bmatrix} \qquad \mathbf{f} = \begin{Bmatrix} \mathbf{f^{ext}} \\ \mathbf{0} \\ \mathbf{0} \end{Bmatrix}$$

where $\mathbf{a_1}$, $\mathbf{a_2}$, $\mathbf{a_3}$ are vectors with the modal contribution of the impacted floor, the non-impacted floor and the wall respectively. Matrices $\mathbf{D_{ii}}$ and $\mathbf{B_{ij}}$ have the same structure as in the previous section. In this case each plate is linked to the other two, therefore the global matrix is full.

4 Lightweight floors

The second model developed deals with impact noise in lightweight floors. A popular configuration for lightweight floor structures is considered, consisting of two leaves of material (generally plasterboard) connected by steel studs (as considered in Takahashi [28]). These studs, aside from providing structural performance, also create an unwanted vibration transmission path connecting the two leaves.

The vibration transmission between the leaves is an important parameter in order to understand the structural behaviour of the floor. An important output of interest is then the vibration level difference D_{ij} between the upper and the lower leaves, as defined by Hopkins [19] and shown by Gerretsen [16, 15].

4.1 Studs: meaning and modelling

This type of floors, as they are comprised of two rectangular leaves, can be modelled using plate theory. It has also been shown by Poblet-Puig *et al.* [23] that it is possible to use springs to represent the studs that connect them in order to further simplify the model. Either translational or rotational springs may be used to reproduce the behaviour of real studs with a fitting of frequency-dependent stiffness. Some 2D models about the effect of different shapes of studs in the vibration level difference on lightweight floors are presented in [23] and simplified models as those shown in Fig. 5 are validated by comparing them with finite element analyses that consider the shape of the studs.

The use of modal analysis to deal with lightweight floors as shown here takes into account the effect of the third dimension, and shows the differences between having point or line connections between plates and studs.

In addition, studies have been made in the literature into two different methods of modelling the stud connections which link the two plates. Either they can be modelled as point connections, where each point represents one of the screws that connects the leaf to the stud, or they can be represented as line connections, where one spring acts along the length of the stud.

In total, three structural models are developed. A simplified diagram of each is shown in Fig. 5.

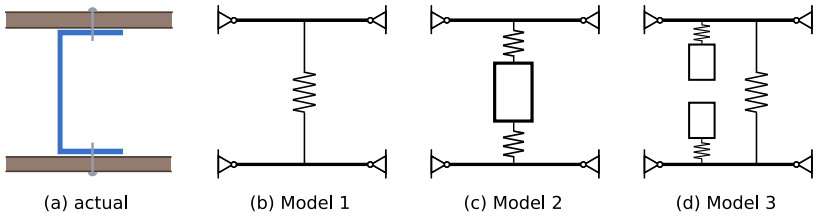

Figure 5: The three models and a sketch of the physical reality.

All models feature two plates, upper (plate 1) and lower (plate 2), which model the leaves of the floor. In Model 1, these plates are connected by a spring which represents the stud. The stiffness of the spring models the stud's cross-sectional flexibility, which causes the vibration transmission from plate 1 to plate 2. The stiffness of the stud in bending is not taken into account.

Model 2 introduces a beam, computed using modal analysis, which connects the plates via two springs, one for the upper plate and one for the lower plate. The springs here represent the flexibility of the contact between the plates and the stud, while the bending stiffness of the stud and the effect of its mass is modelled by the beam. This configuration neglects the cross-section flexibility.

Model 3 combines the first two models. The main transmission path is a spring that connects the two plates and represents the stud's cross-sectional flexibility. In addition, a beam is connected to each plate so that the mass and bending stiffness of the stud are not neglected.

4.2 Model 1: plates and springs

4.2.1 Point connections

The first model consists of two plates connected by a spring. This situation has also been considered by Chung and Emms [8] and Sjökvist *et al.* [27, 26].

The effect of a single connection at co-ordinates (x_r, y_r) is considered to begin with, as shown in Fig. 6.

With the sign conventions shown in Fig. 6, the forces on the plates, F_1 and F_2, are given by

$$F_1 = -F_2 = -K(u_1 - u_2) = -K\left(\sum_{pq} a_{pq}^{(1)}\psi_{pq}(x_r, y_r) - \sum_{pq} a_{pq}^{(2)}\psi_{pq}(x_r, y_r)\right), \quad (18)$$

where K is the stiffness of the spring, $a_{pq}^{(1)}$ are the coefficients of the upper plate and $a_{pq}^{(2)}$ are the coefficients of the lower plate. ψ_{pq} are the mode shapes of the plates, as defined in Eq. (4).

The force term of each plate equation should now be adapted to include the excitation force from the spring, and hence the two equations describing the upper and lower plates can be written in matrix form as

$$\begin{bmatrix} \mathbf{D_{11}} + K\mathbf{C_{11}} & -K\mathbf{C_{12}} \\ -K\mathbf{C_{21}} & \mathbf{D_{22}} + K\mathbf{C_{22}} \end{bmatrix} \begin{Bmatrix} \mathbf{a_1} \\ \mathbf{a_2} \end{Bmatrix} = \begin{Bmatrix} \mathbf{f^{ext}} \\ \mathbf{0} \end{Bmatrix} \quad (19)$$

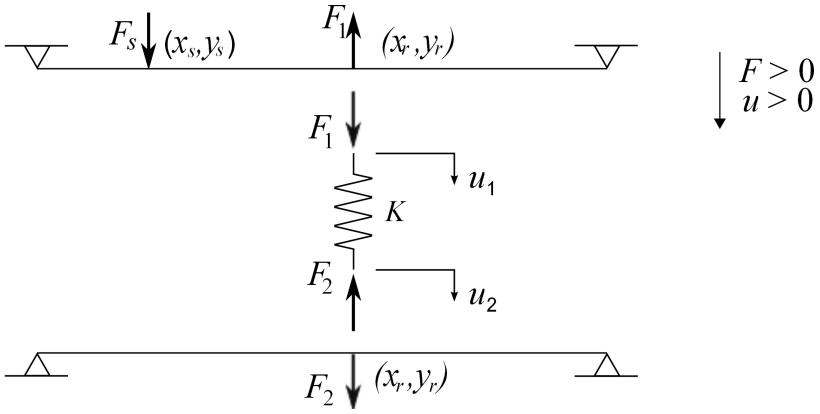

Figure 6: Force diagram of the two leaves connected by a single point spring.

where matrices $\mathbf{D_{ii}}$ have already been defined in Section 3 and matrices $\mathbf{C_{ij}}$ are due to the spring effect which causes a force proportional to the displacement of the plate. Their elements are the product of the shape function associated to the plate i times the shape function associated to the plate j both evaluated at point (x_r, y_r).

The equations are easily modified to take into account more than one connecting spring: more force terms have to be added into the modified weak form of the plate equation:

$$F_1 = -F_2 = -\sum_{j=1}^{ns} \left[K \left(\sum_{pq} a_{pq}^{(1)} \psi_{pq}^{j} - \sum_{pq} a_{pq}^{(2)} \psi_{pq}^{j} \right) \right], \tag{20}$$

where ns is the number of springs to be added, and ψ^j and ψ^j are the mode shapes evaluated at the position of spring j.

4.2.2 Line connections

In order to model line connections, the force due to the spring F_r acts on a line running across the plate in the x-direction, at a distance y_r from the plate edge and is a function of x, given by

$$F_r(x) = K_L \left[\sum_{pq} a_{pq}^{(1)} \psi_{pq}(x,y) - \sum_{pq} a_{pq}^{(2)} \psi_{pq}(x,y) \right], \tag{21}$$

where K_L is the stiffness of the spring per unit length.

The equations for a line spring are therefore very similar to the point spring ones, except that the entries in matrices $\mathbf{C_{ij}}$ must be integrated with respect to x (which can be done analytically for a simply supported plate), and the spring stiffness, K, becomes K_L, the stiffness of the spring per unit length.

4.3 Plates, beams and springs

In order to take into account the mass of the studs, as well as any effects that the studs' bending stiffness may have on the vibration of the plates, two models are developed including beams analysed with modal analysis.

To analyse the beams, the Euler-Bernoulli beam equation

$$EI\frac{\mathrm{d}^4u(x)}{\mathrm{d}x^4} - \rho_l\omega^2 u(x) = q(x) \tag{22}$$

is used. The process is similar to that used earlier for the plate equation. The beams, too, are assumed to be simply supported and deflection is described by a sine series, in this case

$$u(x) = \sum_{i=1}^{N} b_i\chi_i(x) \tag{23}$$

where b_i are the modal contributions of each function, $\chi_i(x) = \sin\left(\frac{i\pi x}{L}\right)$ and L is the length of the beam.

4.3.1 Model 2: beam connection

At this stage, the springs are considered to be point springs. The extra structural element means that as well as one equation for each of the plates, the final system also has an equation describing the motion of the beam. To obtain it, the beam equation is modified to include the effects of two springs: one connecting the beam to the upper plate and one to the lower plate. This results in

$$\begin{aligned}
&\left(EI\,k_i^4 - \rho_l\omega^2\right)\left(\int_x \chi_i^2\,\mathrm{d}x\right) b_i = \\
&= K\,\chi_i(x_r,y_r)\left(\sum_{pq} a_{pq}^{(1)}\psi_{pq}(x_r,y_r) - \sum_j b_j\chi_j(x_r,y_r)\right) - \\
&-K\,\chi_i(x_r,y_r)\left(\sum_j b_j\chi_j(x_r,y_r) - \sum_{pq} a_{pq}^{(2)}\psi_{pq}(x_r,y_r)\right),
\end{aligned} \tag{24}$$

where ψ and χ are the plate and beam mode shapes respectively, and $\mathbf{a_1}$, $\mathbf{a_2}$ and $\mathbf{b}$ are the vectors of coefficients for the upper plate, the lower plate and the beam respectively.

In matrix form, the equations governing the whole system (including plates) can be written as

$$\begin{bmatrix} \mathbf{D_{11}} + K\mathbf{C_{11}} & -K\mathbf{C_{1b}} & \mathbf{0} \\ -K\mathbf{C_{b1}} & \mathbf{D_{bb}} + 2K\mathbf{C_{bb}} & -K\mathbf{C_{b2}} \\ \mathbf{0} & -K\mathbf{C_{2b}} & \mathbf{D_{22}} + K\mathbf{C_{22}} \end{bmatrix} \begin{Bmatrix} \mathbf{a_1} \\ \mathbf{b} \\ \mathbf{a_2} \end{Bmatrix} = \begin{Bmatrix} \mathbf{f^{ext}} \\ \mathbf{0} \\ \mathbf{0} \end{Bmatrix} \tag{25}$$

where subscript b means beam. Matrices $\mathbf{D_{ii}}$ have been already defined and matrix $\mathbf{D_{bb}}$ is analogous but for the beam (with its own 1D shape functions). $\mathbf{C_{ib}}$ and $\mathbf{C_{bi}}$ are matrices caused by the interaction between the beam and plate i and their elements are the product of the shape function associated to the plate i times the shape function associated to the beam both evaluated at point (x_r, y_r). Matrices $\mathbf{C_{ii}}$ have already been described after Eq. (19) and $\mathbf{C_{bb}}$ is analogous but with the beam shape functions.

4.3.2 Model 3: beam and spring connection

A model combining the two previous approaches is used. The cross-sectional stiffness is accounted for by a spring which couples the two leaves of the floor directly. In addition, each leaf is connected to a beam, which accounts for the stud's bending stiffness and mass.

Now, three forces act on the upper plate: the excitation force, the force from the beam, and the force from the lower plate. Assuming that these are all point forces, the equation for the upper plate takes the form

$$\left(\int_\Omega \psi_{pq}^2 \,\mathrm{d}\Omega\right)\left(D\,k_{pq}^4 - \omega^2\rho_s\right) a_{pq} = F_s\psi_{pq}^s - F_1\psi_{pq}(x_r, y_r) - F_b\psi_{pq}(x_r, y_r) \tag{26}$$

where F_s is the excitation force,

$$F_1 = K_{aa}(u_1 - u_2) = K_{aa}\left(\sum_{pq} a_{pq}^{(1)}\psi_{pq} - \sum_{pq} a_{pq}^{(2)}\psi_{pq}\right) \quad \text{and} \tag{27}$$

$$F_b = K_{ab}(u_1 - u_3) = K_{ab}\left(\sum_{pq} a_{pq}^{(1)}\psi_{pq} - \sum_{j} b_{pq}^{(1)}\chi_j\right). \tag{28}$$

The beams have only one force acting on them: the force due to the spring connecting them to the plate. The matrix equations in the simplified form can be written as

$$\mathbf{Ka} = \mathbf{f} \tag{29}$$

where

$$\mathbf{K} = \begin{bmatrix} \mathbf{D_{aa}^{(1)}}+(K_{aa}+K_{ab})\mathbf{C_{aa}^{(1)}} & -K_{ab}\mathbf{C_{ab}^{(11)}} & \mathbf{0} & -K_{aa}\mathbf{C_{aa}^{(12)}} \\ -K_{ab}\mathbf{C_{ba}^{(11)}} & \mathbf{D_{bb}^{(1)}}+K_{ab}\mathbf{C_{bb}^{(1)}} & \mathbf{0} & \mathbf{0} \\ \mathbf{0} & \mathbf{0} & \mathbf{D_{bb}^{(2)}}+K_{ab}\mathbf{C_{bb}}^{(2)} & -K_{ab}\mathbf{C_{ba}^{(22)}} \\ -K_{aa}\mathbf{C_{aa}^{(21)}} & \mathbf{0} & -K_{ab}\mathbf{C_{ab}^{(22)}} & \mathbf{D_{aa}^{(2)}}+(K_{aa}+K_{ab})\mathbf{C_{aa}^{(2)}} \end{bmatrix}$$

$$\mathbf{a} = \begin{Bmatrix} \mathbf{a_1} \\ \mathbf{b_1} \\ \mathbf{b_2} \\ \mathbf{a_2} \end{Bmatrix} \qquad \mathbf{f} = \begin{Bmatrix} \mathbf{f^{ext}} \\ \mathbf{0} \\ \mathbf{0} \\ \mathbf{0} \end{Bmatrix},$$

where $\mathbf{a_1}$ and $\mathbf{a_2}$ correspond to upper and lower leaves and $\mathbf{b_1}$ and $\mathbf{b_2}$ are associated to the upper and lower beams respectively. For matrices $\mathbf{C}$, subscripts a and b are associated to plate and beam respectively showing the type of structures involved in the interaction (and therefore the types of shape functions be multiplied), and superscripts 1 and 2 indicate upper and lower respectively and serve to locate the involved structures.

All matrices have the same form as for the previous models. The system as a whole has two main differences: the positions taken by the coupling matrices in the system matrix, and the fact that here there are two values of stiffness (K_{aa} for the plate-plate connection and K_{ab} for the plate-beam connection).

5 Results and comments

5.1 Simply supported plate

The basic model for a single simply supported plate is tested by comparing it with available experimental data. In [14] the impact noise of a bare concrete floor subjected to the excitation of the tapping machine is measured in the lab. The same experiment is reproduced with the basic model described here.

In [14] the basic geometric data (plate dimensions and thickness) are provided, see Table 1. However, the material properties of concrete are not reported. Due to this, some typical values are used here, see Table 2.

Meaning	**Symbol**	**Value**
Length in the x direction	L_x	2.4 m
Length in the y direction	L_y	2.4 m
Thickness	h	0.1 m

Table 1: Geometric data of the plate provided in [14].

Meaning	**Symbol**	**Value**
Solid density	ρ	2400 kg m^{-3}
Young's modulus	E	30 GPa
Poisson's ratio	ν	0.2

Table 2: Chosen properties of the concrete to complete the necessary data for the model.

Another important parameter is the loss factor of the plate. It is supposed variable with the frequency and its value is interpolated linearly from the values given in [14].

Moreover, in [14] the experimental results are obtained as the average of four different measurements, each one with the tapping machine applied in a different position of the floor, but these positions are not specified.

This situation is reproduced by choosing four different positions and applying the force on them, averaging the power radiated in each case before computing the impact noise pressure level. With the (0, 0) located at a corner of the plate, these positions are: $(0.57\,L_x, 0.57\,L_y)$, $(0.19\,L_x, 0.19\,L_y)$, $(0.19\,L_x, 0.57\,L_y)$, $(0.57\,L_x, 0.19\,L_y)$, see Fig. 7.

For every numerical result shown in this paper the radiated power is obtained by means of the approximation provided by Renji *et al.* [25] for frequencies larger than 560 Hz, and the number of modes M in Eq. (3) is computed such that, for a frequency of computation f, the range of frequencies considered is $f \pm 200$ Hz.

In Fig. 8 the comparison between the basic model and the experimental results is shown. The results are expressed in terms of the normalised impact noise pressure level, averaged in third octave bands.

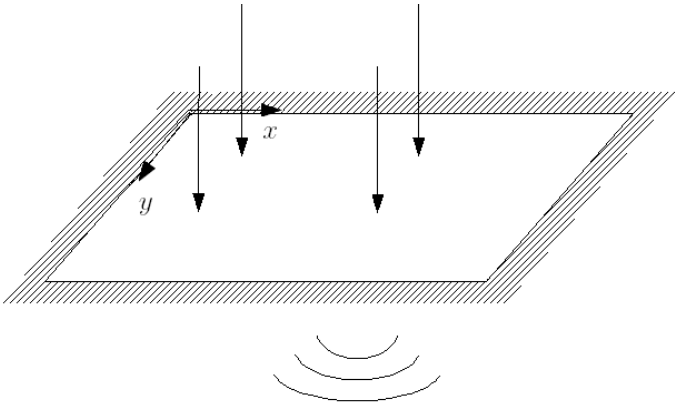

Figure 7: Positions of the applied force

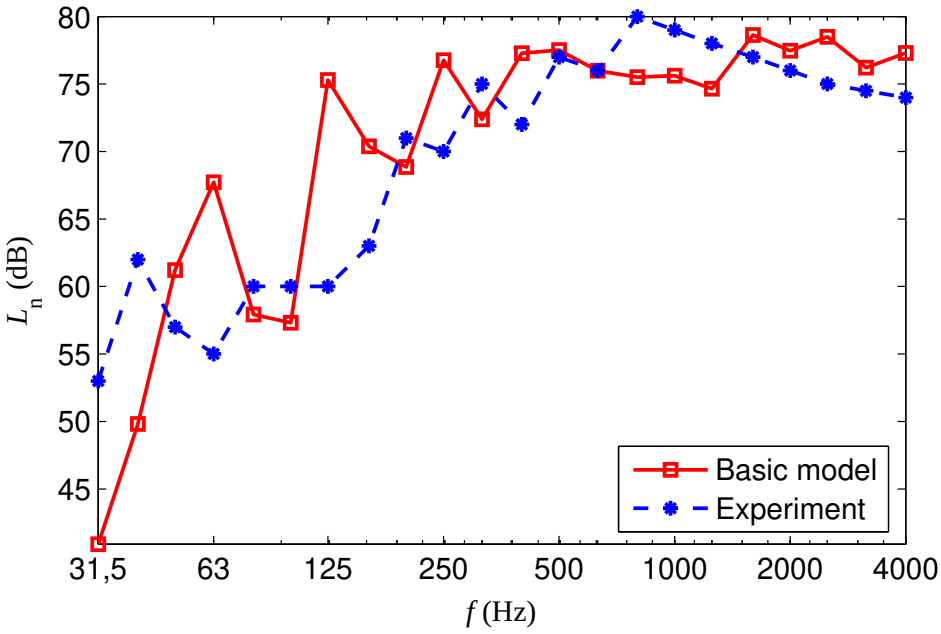

Figure 8: Comparison of the single plate models with experimental measurements

The conclusions drawn from Fig. 8 are that, despite the lack of accurate information about the experiment details (which is reflected in a different influence of the modal density of the plate in both results), the trend of the results obtained with the model coincides with that of the experimental values.

5.2 Flanking transmission

5.2.1 Vibration transmission in continuous floors

The case shown in Fig. 3 is analysed. The properties of the plates are defined in Table 3.

The influence of the rotation stiffness of the joints in the noise propagation along

plates is studied here. The force is applied in the first plate and the impact noise levels below every plate are computed. The results are expressed in terms of the adjusted normalised impact noise pressure level.

Meaning	**Symbol**	**Value**
Plate dimensions	L_x, L_y	2.4 m × 2.4 m
Plate thickness	h	0.1 m
Solid density	ρ	2400 kg m^{-3}
Young's modulus	E	30 GPa
Poisson's ratio	ν	0.2
Loss factor	η	1.5%

Table 3: Plate properties

The value of k_θ is modified in order to check its influence in the impact noise level below the plates, leaving the other parameters unchanged. The force is applied only in the first plate and, considering the $(0, 0)$ as located at a corner of the plate, application points are: $\left(\frac{L_x}{2}, \frac{L_y}{2}\right)$, $\left(\frac{L_x}{4}, \frac{L_y}{4}\right)$, $\left(\frac{L_x}{4}, \frac{L_y}{2}\right)$, $\left(\frac{L_x}{2}, \frac{L_y}{4}\right)$. The resulting powers are averaged before computing the impact noise level.

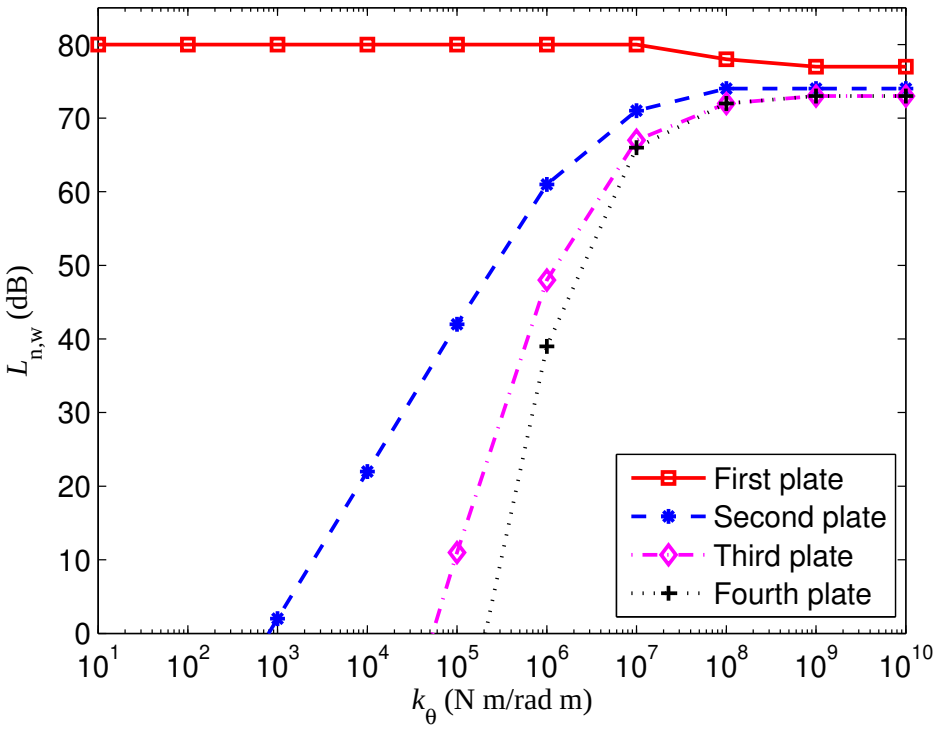

Figure 9: Dependence of the normalised impact noise level on the rotation stiffness of the joints

The results in Fig. 9 show the large influence of the rotation stiffness of the joints

in the transmission of the impact noise along the floor. For low values of the stiffness, the transmission of the impact noise along the floor is almost zero. As the stiffness increases, the radiated power tends to be distributed along the plates, and the power radiated by each plate is almost the same for large values of the stiffness.

5.2.2 Vibration transmission in T-shaped joints

The case shown in Fig. 4 is presented here. The two wall-floor stiffnesses are taken equal ($k_{\theta 13} = k_{\theta 23}$), whereas a different value of the floor-floor stiffness ($k_{\theta 12}$) is used.

The influence of the floor-wall flanking transmission for different fixed values of the floor-floor flanking transmission (10 N m/rad m, 10^4 N m/rad m, 10^7 N m/rad m and 10^{10} N m/rad m) is analysed, in order to consider every case from a very flexible connection between floors to a continuous floor (very stiff connection).

For each case, the impact noise level obtained in both rooms is computed for different values of the stiffness of the floor-wall connection $k_{\theta 13} = k_{\theta 23} = k_\theta$.

In Fig. 10 the adjusted normalised impact noise pressure level for each room and each value of k_θ is shown for the four mentioned cases. The plates characteristics and the application points of the force are the same as defined in Section 5.2.1, and the impact is applied only in the floor above first room. If the connection between the impacted and the unimpacted floor is stiff enough as to transmit most of the vibration (Fig. 10 d), the effect of the floor-wall flanking transmission is not important enough for causing significant differences in the impact noise perceived in both rooms. However, if the stiffness of the floor-floor connection is small, and consequently the floor-floor flanking transmission is low (Fig. 10 a), the influence of the floor-wall flanking transmission increases considerably.

5.3 Lightweight floors

For the case of lightweight floors, some examples and validation tests are presented. In them, the leaves are assumed to have the properties of GN plasterboard as given in Table 4 and the plate excitation is a constant, frequency independent force of 1 N applied at point (x=0.5 m, y=0.5 m), assuming than the (0,0) is located in a corner. The translational stiffness of the springs modelling the studs is assumed to be $K_L = 10^6$ N m^{-2} for line connections, and the stiffness of point springs is calculated according to

$$K = \frac{L_x K_L}{n}, \tag{30}$$

where n is the number of point connections per stud, with the aim of having the same total stiffness over the whole plate for both point and line connections.

5.3.1 Validation of Model 1

Craik [9] describes a method of estimating the vibration level difference, D_{ij}, in a two-leaf lightweight panel by using statistical energy analysis (SEA). The value is computed using the equation

$$D_{12} = 10 \log_{10} \left(\frac{\langle |v_{\mathrm{upper}}|^2 \rangle}{\langle |v_{\mathrm{lower}}|^2 \rangle} \right) = 10 \log_{10} \left[\rho_{s2} \eta_2 \omega \frac{|Y_1 + Y_2 + Y_t|^2}{n \mathrm{Re}(Y_2)} \right], \tag{31}$$

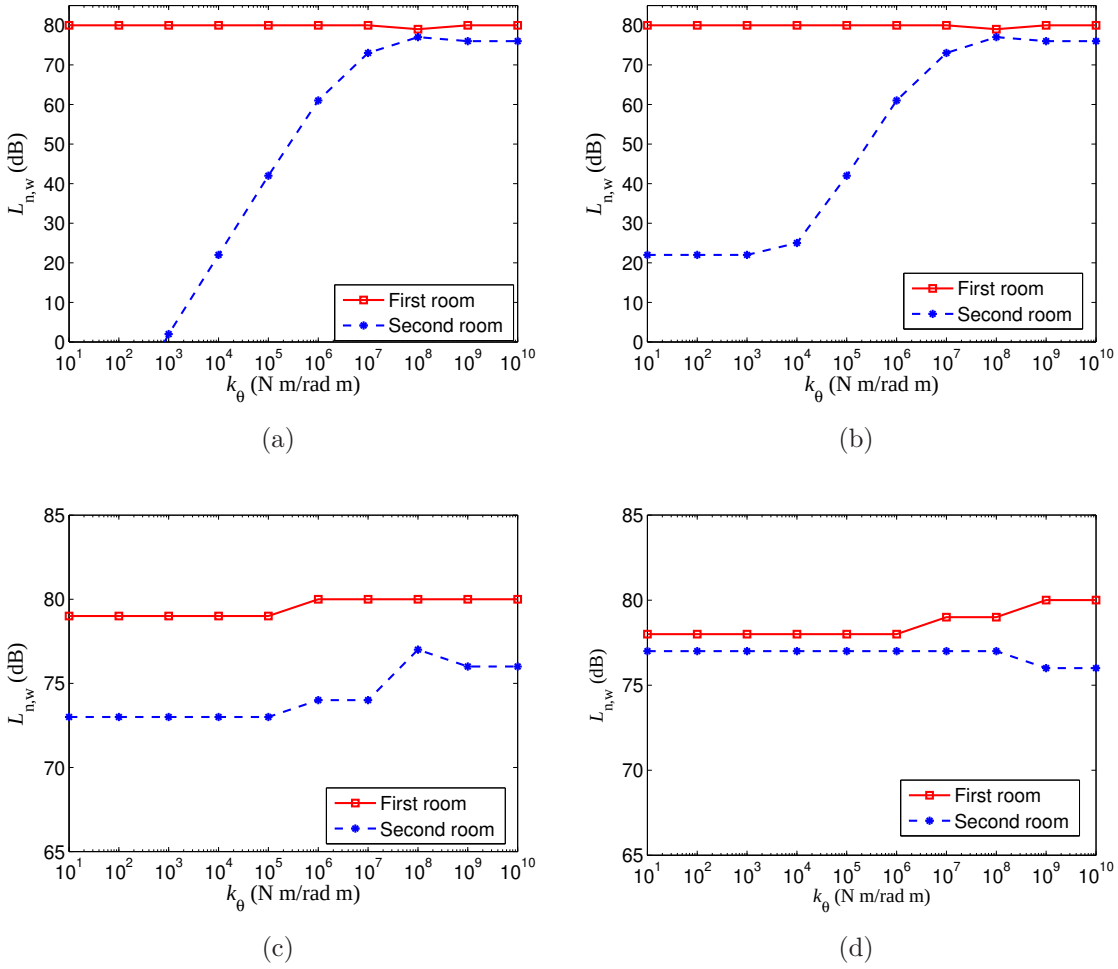

Figure 10: Dependence of the normalised impact noise level calculated in each room on the rotation stiffness of the wall-floor connection. (a): $k_{\theta 12} = 10$ N m/rad m (b): $k_{\theta 12} = 10^4$ N m/rad m (c): $k_{\theta 12} = 10^7$ N m/rad m and (d): $k_{\theta 12} = 10^{10}$ N m/rad m

Variable	**Symbol**	**Value**
Plate size, x direction	L_x	2.4 m
Plate size, y direction	L_y	2.4 m
Thickness	h	0.013 m
Young's modulus	E_{plate}	2.5×10^9 N m^{-2}
Density	ρ_{plate}	692.3 kg m^{-3}
Poisson's ratio	ν	0.3
Loss factor	η	3%

Table 4: The assumed properties for a GN plasterboard leaf, used for all analyses.

where ρ_s is the plate density per unit area, η is the damping factor, ω is the frequency, Y is the plate structural input mobility, and n is the number of point connecting ties per unit area. Y_t is the mobility of a point connecting tie; for a spring of stiffness K_t,

$Y_t = \mathrm{i}\omega/K_t$. The subscripts 1 and 2 refer to the upper and lower plates, respectively.

Fig. 11 shows the results obtained with Model 1 along with the results obtained using SEA for a plate as defined in Table 4 when the above-mentioned force of 1 N is exerted on it. In both cases, point springs are used to model the connections between plates.

SEA has been chosen as a reference for the validation of the results because it is such a widely used technique in the field of acoustics and allows to establish a reference trend without much computational effort.

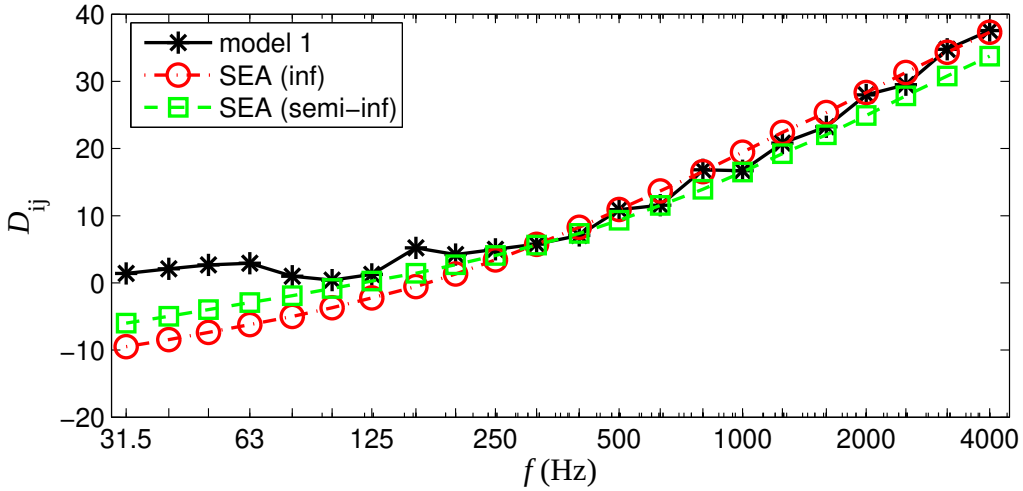

Figure 11: Comparison of Model 1 and two similar SEA models, for a system of 3 studs × 7 screws per stud = 21 spring point connections.

Cremer *et al.* [12] give two equations for determining the structural mobilities of the plates; one for an infinite plate and one for a semi-infinite plate. At higher frequencies, the results computed using Model 1 lie between those computed with these two methods. At lower frequencies results differ, but those obtained with the developed model are more consistent with typical experimental results than those obtained with SEA. SEA provides values of D_{ij} lower than zero and this does not happen in experiments unless resonance phenomena appear. Besides, the lack of accuracy of SEA methods for low frequencies is well known, since the required hypotheses of the method are not fulfilled at those frequencies.

5.3.2 Point and line connections

Fig. 12 shows the vibration level difference computed with Model 1 for both line connections and point connections with various spacings. In all cases, studs are spaced at 600 mm centres. The plates properties and the force type are the same as defined in Section 5.3.1.

Craik and Smith [10] have suggested that line connections are only applicable for low frequencies, or when the connecting screws are sufficiently close together. Fig. 12 shows that, as the number of screws per stud increases, results tend towards those

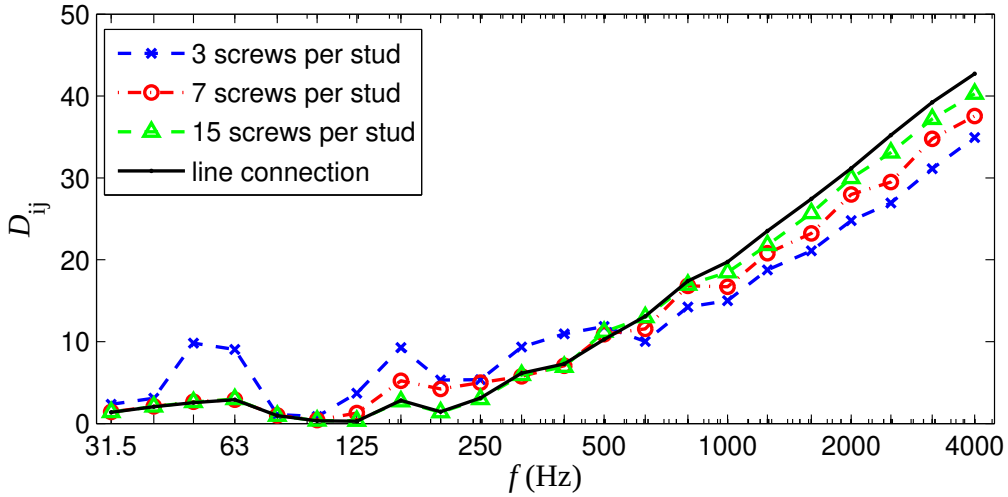

Figure 12: Vibration level difference for various spring arrangements (Model 1).

obtained using a line connection. However, for frequencies higher than a certain value (around 500 Hz), the studs with higher screw spacings lead to a lower vibration level difference. This is because the wavelengths for higher modes (which govern the results at high frequencies) are shorter, and therefore fit between screws if they are spaced far enough apart. In this case the plate can vibrate freely between the screws without restraint and there is a higher level of vibration (and therefore a smaller vibration level difference).

Fig. 13 shows plots of the velocity field across the plate for $f = 1000\,\mathrm{Hz}$. The effect of the screws on the shape of the velocity field of each leave can be seen. For the excited plate, the influence of the springs in shown in the appearance of two main directions of propagation from the point of force application. For the non-excited one, the distribution of the vibration across the plate is a result of the transmission through the springs.

5.3.3 Border effect

The influence of the position of the stud is taken into account here. Fig. 15 shows the vibration level difference computed with Model 1 for two situations: a stud located in the middle of the plate, and a stud located in an edge of the plate.

In order to capture the effect of the latter situation, the only difference with previous cases is that a different basis of functions is used. The eigenfunctions of a plate with three simply supported edges and a free edge reviewed by Leissa [21] are used as interpolation functions:

$$\Psi_{pq} = \begin{cases} \left(\sin\frac{p\pi x}{L_x}\right)\left(1-\frac{y}{L_y}\right) & \text{for } q=1 \\ \left(\sin\frac{p\pi x}{L_x}\right)\left(\sin\left[\gamma_2(\frac{y}{2L_y}-\frac{1}{2})\right]+\frac{\sin(\gamma_2/2)}{\sinh(\gamma_2/2)}\sinh\left[\gamma_2(\frac{y}{2L_y}-\frac{1}{2})\right]\right) & \text{for } q>1 \end{cases} \tag{32}$$

where the values of γ_2 are obtained as roots of

$$\tan\gamma_2/2 - \tanh\gamma_2/2 = 0.$$

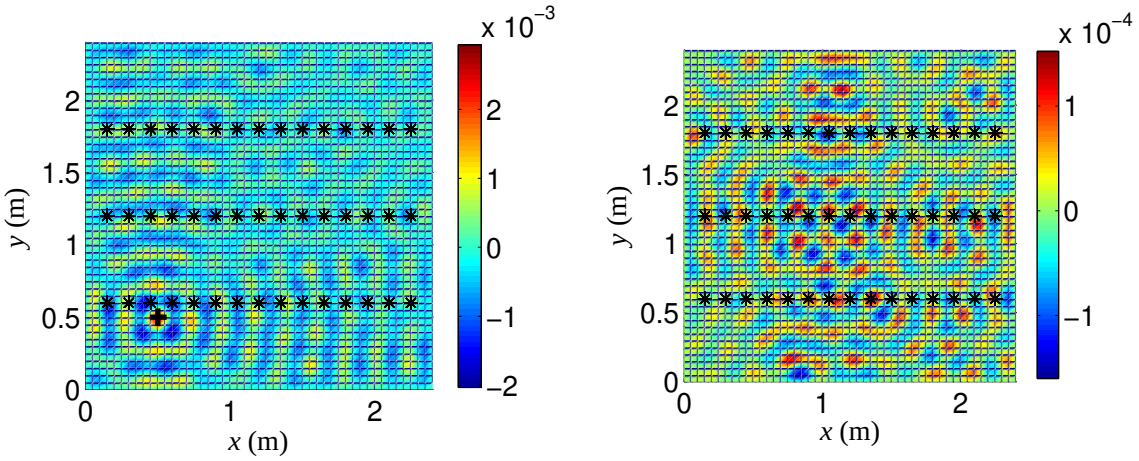

Figure 13: Velocity field in upper (left) and lower (right) plates with 15 screws on each stud for $f = 1000\,\text{Hz}$. Screws denoted by *, force denoted by + (note the different scales for the upper and lower leaves, both in m s^{-1})

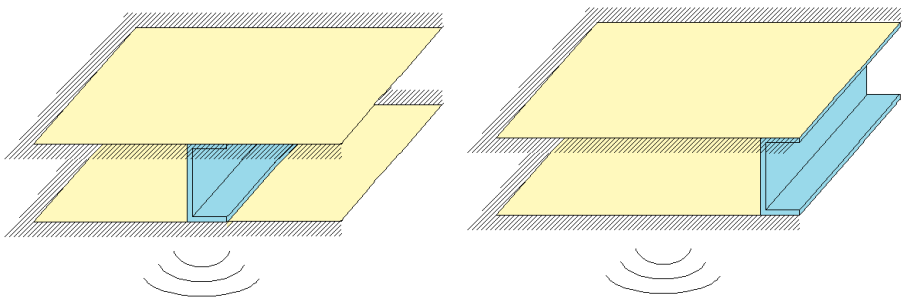

(a) (b)

Figure 14: Situations taken into account. (a): stud at the center and (b): stud at the border

The stud is placed in the free edge to consider the case of the stud located in an edge. Fig. 14 shows an schematic view of the new problem. The properties of the plates and the type of force are the same as defined in Section 5.3.1.

According to Fig. 15, the location of the studs has a significant influence in the vibration level difference. A stud located in the edge of the plate provides a larger noise transmission than another one located in the middle of the plate. This result is coherent with the expressions shown in [18], assuming the case of the stud in the middle comparable to the infinite plate situation and the case of the stud in the edge to that of the semi-infinite plate.

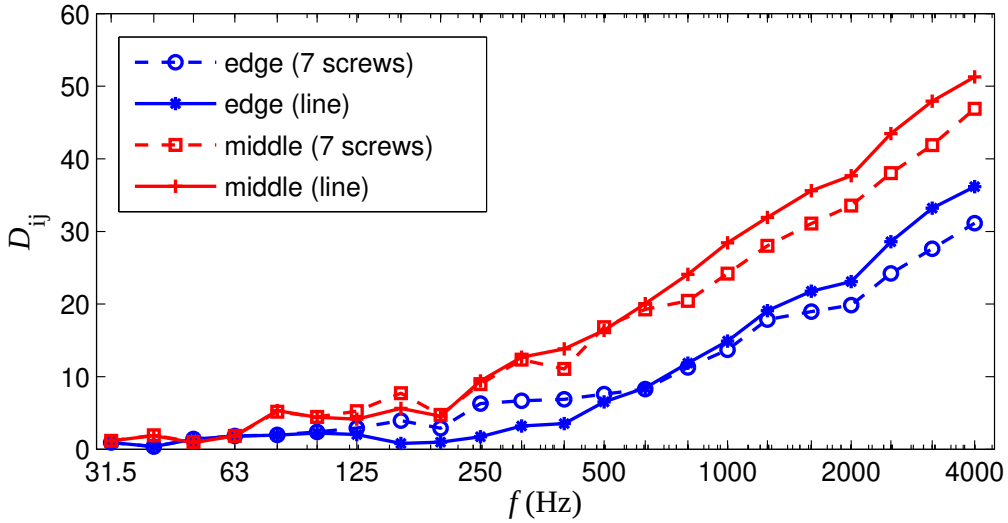

Figure 15: Vibration level difference for two positions of the stud. The plate has a free edge.

5.3.4 Comparison of the three models

The three configurations used to model the studs are compared. The vibration level difference for all three models is shown in Fig. 16. The results obtained with SEA are also shown on the plot.

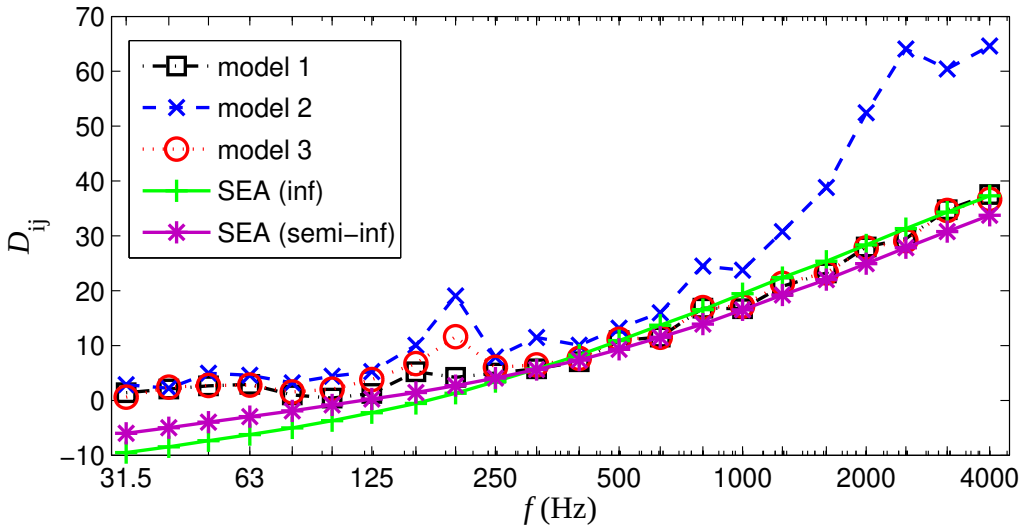

Figure 16: Vibration level difference for the three models. Two SEA models are also shown for comparison.

Models 1 and 3 give similar predictions, and both agree well with SEA, while Model 2 predicts a higher vibration level difference. This happens because Model 2

uses a different vibration transmission path to the other two models. This would be suitable for studs with a very rigid cross-section (as solid wood studs) with elastic contacts between plates and studs, which is not the case. For the considered value of the spring stiffness, Model 2 overestimates the stiffness of the transmission path.

In this specific case it would be better to use either Model 1 or Model 3. The difference between them is that in Model 3 the stiffening effect of the stud is more relevant. For cases like the developed one, where the cross flexibility predominates, both models provide good results and, taking into account the increment of the number of degrees of freedom required by Model 3, the recommended model for this particular situation would be Model 1.

6 Conclusions

The modal bases used for solving analytically the dynamics equation in rectangular plates have been used here for dealing with more complex configurations of floors. Impact noise has been computed in a deterministic way for different floors along the entire frequency range. For lightweight floors and flanking transmissions impact noise can be modelled through this technique and the validation test shows a good agreement of the results.

For the case of floors with elastic joints, the insulating effect of these devices has been shown. For instance, a joint with a rotation stiffness of 10^5 N m/rad m provides a reduction of the order of 40 dB in adjacent floors.

For the modelling of lightweight floors, three models have been presented. Models 1 and 3 are characterised by having a spring as the transmission path between plates. Model 2 has also a beam in the transmission path. Validation of these models with SEA results leads to the conclusion that the addition of a beam in the transmission path overestimates the vibration level difference between plates for the spring stiffness considered. Therefore, the recommended model for light metal studs in double walls is Model 1, since it provides results very similar to Model 3 with less degrees of freedom.

The influence of having point or line connections between plates and studs has been studied with the developed method. For low frequencies the modal behaviour of the plate shows no difference between having line connections or many point connections. However, when the frequency value exceeds a certain threshold (about 500 Hz), the behaviour of the plate for both types of connections differs. This disagreement for high frequencies coincides with the point raised by Craik *et al.* [10].

The last application of the modal analysis technique has been the study of the stud position influence in the vibration level difference. The transmission of the vibration between plates has proven to be larger for a stud located in the edge than for a centered stud.

In summary, the main advantage of this method is the possibility of analysing different configurations of floors with a reasonable computational cost and good results for the whole frequency range. Other configurations of floors can be modelled by changing the basis of functions (for imposing free or clamped edges) or adding information to the weak form (to apply conditions in bending moments or forces). Also other types of stud models can be used, such as those shown by Poblet-Puig *et*

al. [23] consisting on springs with frequency-dependent stiffness.

Acknowledgements

The financial support of the Ministerio de Ciencia e Innovación (BIA2007-66965, DPI2007-62395), the Ministerio de Educación y Ciencia (FPU scholarship program), the Universitat Politècnica de Catalunya and the Col·legi d'Enginyers de Camins, Canals i Ports is gratefully acknowledged.

References

[1] *ISO 717-2:1997, Acoustics – Rating of sound insulation in buildings and of building elements – Part 2: Impact sound isolation.* Geneva, Switzerland, 1997.

[2] *ISO 140-6:1998, Acoustics – Measurement of sound insulation in buildings and of building elements – Part 6: Laboratory measurements of impact sound insulation of floors.* Geneva, Switzerland, 1998.

[3] *ISO 140-7:1998, Acoustics – Measurement of sound insulation in buildings and of building elements – Part 7: Field measurements of impact sound insulation of floors.* Geneva, Switzerland, 1998.

[4] L.L. Beranek and I.L. Vér. *Noise and vibration control engineering: Principles and Applications.* Wiley, 1992.

[5] A. Berry, J.L. Guyader, and J. Nicolas. A general formulation for the sound radiation from rectangular, baffled plates with arbitrary boundary conditions. *J. Acoust. Soc. Am.*, 88(6):2792–2802, 1990.

[6] J. Brunskog and P. Hammer. The interaction between the ISO tapping machine and lightweight floors. *Acta Acust. United Acust.*, 89(2):296–308, 2003.

[7] J. Brunskog and P. Hammer. Prediction model for the impact sound level of lightweight floors. *Acta Acust. United Acust.*, 89:309–322, 2003.

[8] H. Chung and G. Emms. Fourier series solutions to the vibration of rectangular lightweight floor / ceiling structures. *Acta Acustica United with Acustica*, 94(3):401–409, 2008.

[9] R.J.M. Craik. *Sound transmission through buildings using statistical energy analysis.* Gower Publishing Ltd., 1996.

[10] R.J.M. Craik and R.S. Smith. Sound transmission through double leaf lightweight partitions part II: airborne sound. *Appl. Acoust.*, 61(2):247–269, 2000.

[11] Robert J. M. Craik and Robin Wilson. Sound transmission through parallel plates coupled along a line. *Appl. Acoust.*, 49(4):353–372, 1996.

[12] L. Cremer, M. Heckel, and E.E. Ungar. *Structure-borne sound*. Springer-Verlag, 1973.

[13] F. Fahy. *Sound and structural vibration*. Academic Press, 1989.

[14] R.D. Ford, D.C. Hothersall, and A.C.C. Warnock. The impact insulation assessment of covered concrete floors. *J. Sound Vib.*, 33(1):103–115, 1974.

[15] E. Gerretsen. Calculation of the sound transmission between dwellings by partitions and flanking structures. *Appl. Acoust.*, 12(6):413–433, 1979.

[16] E. Gerretsen. Calculation of airborne and impact sound insulation between dwellings. *Appl. Acoust.*, 19(4):245–264, 1986.

[17] K.F. Graff. *Wave motion in elastic solids*. Dover Publications, 1991.

[18] C. Guigou-Carter and M. Villot. Analytical and experimental study of single frame double wall. Euronoise proceedings, 2006. The Acoustical Society of Finland and VTT.

[19] C. Hopkins. *Sound insulation*. Elsevier Ltd., 2007.

[20] P. Jean and J.F. Rondeau. A simple decoupled modal calculation of sound transmission between volumes. *Acta Acust. United Acust.*, 88(6):924–933, 2002.

[21] A.W. Leissa. *Vibration of plates*. Acoustical Society of America, 1993.

[22] R. H. Lyon. *Statistical Energy Analysis of Dynamical Systems*. M.I.T. Press, 1975.

[23] J. Poblet-Puig, A. Rodriguez-Ferran, C. Guigou-Carter, and M. Villot. The role of studs in the sound transmission of double walls. *Acta Acust. United Acust.*, 95(3):555–567, 2009.

[24] A. Rabold, A. Düster, and E. Rank. FEM based prediction model for the impact sound level of floors. In *Proceedings of acoustics'08 Paris*, pages 2993–2998, 2008.

[25] K. Renji, P. S. Nair, and S. Narayanan. On acoustic radiation resistance of plates. *J. Sound Vib.*, 212(4):583–598, 1998.

[26] L.-G. Sjökvist, J. Brunskog, and F. Jacobsen. Parameter survey of a rib stiffened wooden floor using sinus modes model. In *Proceedings of acoustics'08 Paris*, pages 3011–3015, 2008.

[27] L.G. Sjökvist and J. Brunskog. Modal analysis for floors in lightweight buildings. Proceedings of internoise, 2007. Istanbul, Turkey.

[28] D. Takahashi. Sound radiation from periodically connected double-plate structures. *J. Sound Vib.*, 90(4):541–557, 1983.

[29] I.L. Vér. Impact noise isolation of composite floors. *J. Acoust. Soc. Am.*, 50(4):1043–1050, 1971.

[30] E.G. Williams. A series expansion of the acoustic power radiated from planar sources. *J. Acoust. Soc. Am.*, 73(5):1520–1524, 1983.